View metadata, citation and similar papers at core.ac.uk

brought to you by CORE

provided by JEOS:RP - Journal of the European Optical Society Rapid publications

Tuning the focal point of a plasmonic lens by nematic liquid crystal

M. Bahramipanah
mohsen_bahrami@ee.kntu.ac.ir
Department of Electrical and Computer Engineering, K. N. Toosi University of Technology, Shariati Street, Tehran, Iran

M. S. Abrishamian
Department of Electrical and Computer Engineering, K. N. Toosi University of Technology, Shariati Street, Tehran, Iran

S. A. Mirtaheri
Department of Electrical and Computer Engineering, K. N. Toosi University of Technology, Shariati Street, Tehran, Iran

A theoretical and numerical investigation of tunable plasmonic nano-optic lens on the basis of liquid crystal are proposed as a new method of active modulating the output beam. The focal length can be controlled easily by exposing plasmonic nano-optic lens to constant external electric field. The physical principle of this phenomenon is evaluated from the phase of Fabry-Perot (F-P) resonance in slits and electro-optical effect of liquid crystal. Our numerical simulations reveal that large tuning range of the focal length up to 725 nm can be achieved. The results in this article provide a potential way to realize tunable plasmonic lens, which can be applied as an efficient element in ultrahigh nano-scale integrated photonic circuits for miniaturization and tuning purposes.
[DOI: http://dx.doi.org/10.2971/jeos.2012.12053]

Keywords: Surface plasmons, anisotropic media, tunable nano-optic lens

1 INTRODUCTION

In recent years, optical waveguides that are based on Surface Plasmons (SPs) have triggered an explosion of interest. The unique property of these waveguides is the potential to overcome the diffraction limit in conventional dielectric waveguides as a solution to realize nano-scale photonic devices for high integration [1]. Since the discovery of extraordinary optical transmission (EOT) through a two-dimensional hole array perforated on a metallic film in 1998 [2], there has been a tremendous research effort in the analysis and realization of subwavelength metallic structures. Surface plasmons, excited in metallic surface, have been promoted as the main vector responsible for EOT phenomenon. These researches are considered to be a very promising area for designing new types of nano-optic devices with variant structures in metallic films [3].

A nano-optic device which possesses multifunctional capabilities in shaping and processing an optical beam comprises a variety of subwavelength slits in a metal film or between metal islands. Plasmonic nano-optic lenses that enable superfocusing beyond the diffraction limit have been proposed experimentally as an alternative to the conventional dielectric-based refractive lenses [4]. Metallic nano-optic lenses can implement beam focusing with variable slit depths [5], slit widths [6], geometries [7], and materials [8]. They show great potential for novel applications, ranging from ultrahigh-resolution imaging, single-molecular biosensing, optical data storage, optical-based on-chip analysis to nanolithography.

Due to the dependence of permittivity of metallic materials on frequency, applications of plasmonic nano-optic lenses would be limited because the optical properties of such lenses are not tunable once they are fabricated. Therefore, similar to conventional integrated optics technology, there is a strong requirement for tunability in these devices. Attaining active control of plasmonic signals in nano-optic devices is the greatest challenge that faces SPs researches [9, 10]; and most research studies in this field are still at an early stage.

Previous studies show that there are several methods to implement beam manipulation including nonlinear optical phased arrays [11, 12], solid crystal based electro-optic modulators [13], acousto-optic modulators [14], micro-electromechanical (MEMs) actuators [15], and liquid crystal (LC) optical phased arrays [16]. However, the high pump intensity of the optically tunable method and the slow response time of mechanically and thermally tunable methods have restricted the practical applications of beam manipulating devices.

Recently, the effect of anisotropic layer modulation on the surface plasmon dispersion, the related optical transmission and the underlying mechanism is proposed experimentally [17]. Anisotropic materials, due to their fundamental feature of providing controllable birefringence, are useful in optics and proposed as switches [18, 19], filters, beam deflector, etc. in various applications [20]-[23]. Therefore, we have proposed a novel plasmonic lens showing the advantages of easy fabrication and electro/magneto tunability by using anisotropic material. Nematic liquid crystal is a kind of

Received June 14, 2012; revised ms. received September 15, 2012; published December 22, 2012 ISSN 1990-2573

birefringent materials with an optical axis associated with the macroscopic orientation or director of the molecules and the ease with which their molecules will change alignment in response to an outside stimulus. Anisotropic media like nematic liquid crystal are used to modulate the phase of incident light. Upon applying a voltage, the molecules tilt and cause the incident light to face a change in refractive index. The change in refractive index translates directly to a change in the optical path length and, consequently, a phase shift for the incident light and, consequently, affects the propagation of SPPs [24]. With its low driving voltage and low-cost fabrication technology, liquid-crystal technology seems to be a prominent candidate for nano-optic plasmonic lenses.

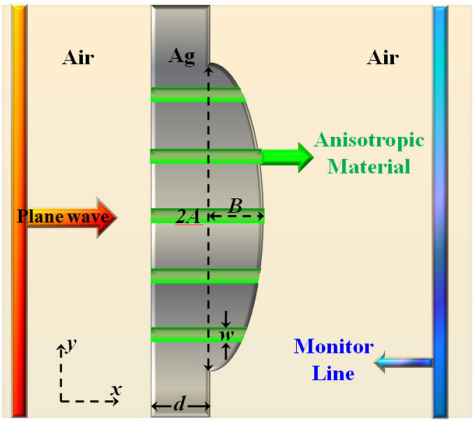

FIG. 1 Tunable nano-optic plasmonic lens

This paper is organized as follows: following this introduction, a brief review of the numerical analysis used in this paper is given in Section 2. Then, results of the detailed simulation of an isotropic nano-optic lens is presented and explained in Section 3. Considering the results of Section 3, a new tunable nano-optic plasmonic lens is proposed in Section 4. In contrast to the previous works, anisotropic material with non-diagonal refractive index tensor, which is close to reality, is utilized in our new proposal. In addition, the effect of changes in tilt angle on the focusing performance of plasmonic lens is analyzed. The focal length can be controlled easily by exposing the plasmonic lens to constant external electric or magnetic field. The dependence of effective refractive index and phase retardation of SPPs propagation in the slits on the misalignments of the liquid crystal molecules, explain the physical principle underlying the phenomenon of active focal length control. Finally, Section 5 concludes the paper.

2 NUMERICAL ANALYSIS

General schematic diagram of a plasmonic lens structure is shown in Figure 1. The structure comprises a nano-slit array that has a convex profile. The convex region, provided on a silver layer of $d = 350$ nm width, is 2 μm wide and accommodates five slits of $w = 80$ nm width with 400 nm slit spacing (center to center) to transmit light with proper phase retardation between aperture elements. The metal thickness is designed to vary in a half-elliptical profile such that the slit depth in the array is 500, 720, 750, 720, and 500 nm from up to down. The lengths of the large and small semi-axis of the elliptic are A = 1 μm and B = 400 nm, respectively. The optical field emanating from a lens can be expressed as Fourier expansion of radiation from infinitesimal dipoles on an exit surface of the lens. The role of the convex lens is to provide a phase correction to each of the Fourier components by virtue of phase retardation resulting from path length difference.

Anisotropic optical material is incorporated in nano-slit array so that the plasmonic lens structure could benefit from the tunability feature. The behavior of EM wave in anisotropic medium is very complex. Numerical methods are preferred in such situation for its simplicity and flexibility. In our analysis, the Anisotropic-Dispersive Finite-Difference Time-Domain (A-D-FDTD) [25, 26] method is employed to illustrate the validity of the tunable plasmonic lens and its new properties. Convolutional perfectly matched layer (CPML) as absorbing boundary condition is also used to dissipate outgoing waves [27]. The simulation dimension is $5 \times 10\ \mu m^2$ and the FDTD grid size and time step are: $\Delta x = \Delta y = 5$ nm and Δt is achieved following the Courant stability condition. Assuming the optical axis of the anisotropic molecules in the $X - Y$ plane, the dielectric tensor of the anisotropic media is as follows [14]:

$$\bar{\bar{\varepsilon}} = \begin{pmatrix} n_0^2 \sin^2(\varphi) + n_e^2 \cos^2(\varphi) & \left(n_0^2 - n_e^2\right) \times \sin(\varphi)\cos(\varphi) & 0 \\ \left(n_0^2 - n_e^2\right) \times \sin(\varphi)\cos(\varphi) & n_0^2 \cos^2(\varphi) + n_e^2 \sin^2(\varphi) & 0 \\ 0 & 0 & n_0^2 \end{pmatrix} \quad (1)$$

The extraordinary (n_e) and the ordinary (n_o) indices of refraction of the anisotropic material are considered to be 1.737 and 1.518, respectively which belong to nematic liquid crystal at room temperature. In Equation 1, ϕ, called tilt angle, is the angle between the optical axis of the anisotropic molecules and the x direction. Moreover, the frequency-dependent complex relative permittivity of silver is characterized by Drude model [28]:

$$\varepsilon(\omega) = \varepsilon_\infty - \frac{\omega_p^2}{\omega^2 + j\gamma\omega} \quad (2)$$

Where $\varepsilon_\infty = 3.7$ is the dielectric constant at infinite angular frequency; $\omega_p = 1.38 \times 10^{16}$ rad/s, the bulk plasma frequency, represents the natural frequency of the oscillations of free conduction electrons; $\gamma = 2.73 \times 10^{13}$ rad/s is the damping frequency of the oscillations; and $\omega$is the angular frequency of the incident electromagnetic radiation.

3 ISOTROPIC PLASMONIC LENS

At this stage, it is assumed that no anisotropic material is used in the structure and all the slits are filled with air. Incident light is a TM polarized plane wave of 850 nm wavelength under the excitation condition of SPPs. In order to investigate the focusing properties and understand the physics underlie

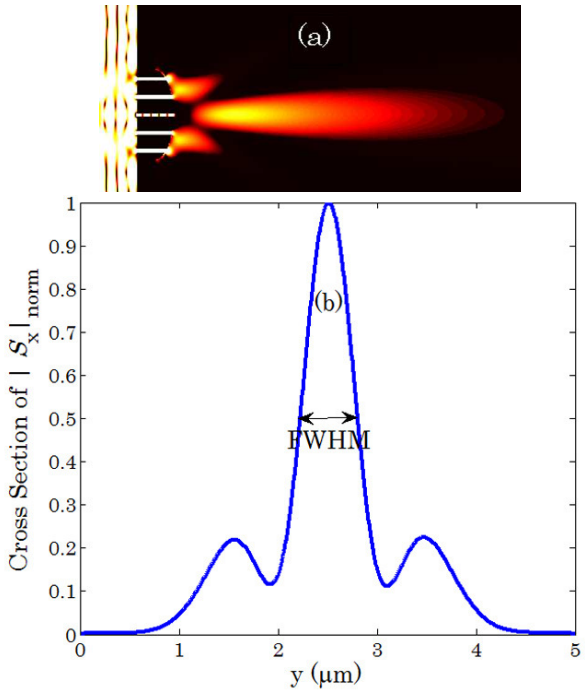

FIG. 2 (a) FDTD calculated result of normalized amplitude of the x-component of the time averaged Poynting Vector $|S_x|$ for designed plasmonic lens at $\lambda = 850$ nm (b) the corresponding calculated cross section of $|S_x|$ at the focal point.

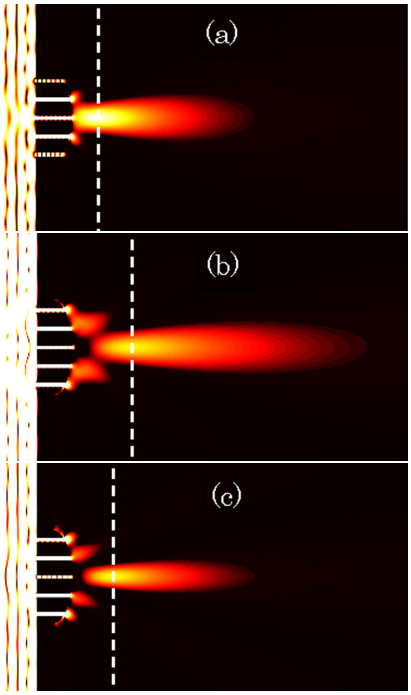

FIG. 3 FDTD calculated results of amplitude of the x-component of the time averaged Poynting Vector $|S_x|$ for (a) $\phi = 0°$ (b) $\phi = 45°$ (c) $\phi = 90°$.

the plasmonic lens structure, the FDTD simulation of amplitude of the x-component of the time averaged Poynting Vector ($|S_x|$) is illustrated in Figure 2(a). As can be seen, this structure focuses a plane wave beam of light at about 1270 nm away from the exit surface. Moreover, the corresponding calculated cross section of $|S_x|$ at focal point is illustrated in Figure 2(b). The focused spot size (full width at half maximum (FWHM)) is about 580 nm. The normalized $|S_x|$ cross section is defined as $|S_x|_{\text{norm}} = \frac{|S_x|}{\text{maximum}(|S_x|)}$.

4 TUNABLE PLASMONIC LENS

There are actually two ways by which the focal point of a plasmonic lens can be shifted. First, the structural parameters of the nano-slits could be altered to satisfy the requirements of phase change. Obviously, this is impractical because different plasmonic lenses should be used to shift the focal point. Second, by changing the optical properties of the material inside the nano-slits, it is possible to shift the focal point. Therefore, at this stage, the nano-slits are stuffed with liquid crystal. The structure is illuminated by a continuous-wave at the wavelength of $\lambda = 850$ nm from the left side of the structure. Changing the optical axis orientation (ϕ) of liquid crystal alters the effective permittivity and, thus, the optical response of the lens. Consequently, the phase retardation through each aperture can then be changed by controlling the voltages and there is no need to change the geometry. The effective refractive index of liquid crystal varies from $n = n_e$ for $\phi = 0$ *degree* to $n = n_o$ for $\phi = 90°$ [14]. The FDTD simulations of amplitude of the x-component of the time averaged Poynting Vector at different tilt angles, $\phi = 0°$, $\phi = 45°$ and $\phi = 90°$, are shown in Figures 3(a-c), respectively. The focal points are illustrated by vertical white dashed lines in x-axis. As shown in Figure 3(a), when the tilt angle is fixed to be $\phi = 0°$, a clear focus appears at about 520 nm away from the exit surface. Then, the structure is illuminated by an external electric field. Therefore, the orientation of the LC molecules alters and a variation in effective refractive index would be discernible. We suppose that the external electric field is enough for changing the tilt angle of the molecules from 0° to 45°. The wavelength of the input signal remains constant and is equal to $\lambda = 850$ nm. In this case, the focus appears at about 1245 nm away from the exit surface as shown in Figure 3(b). If the tilt angle continues to increase to $\phi = 90°$, the focus drops to about 845 nm away from the exit surface which is displayed in Figure 3(c).

In order to find out the reason of the focus moving, the complex propagation constant (β) is obtained from solving the dispersion relation of the metal-anisotropic-metal (MAM) waveguide. The real part of effective refractive index ($\text{Re}(n_{\text{eff}}) = \text{Re}(\beta)/k_0$) of a MAM waveguide versus wavelength is shown in Figure 4 for different tilt angles $\phi = 0°$, $\phi = 45°$ and $\phi = 90°$. As can be seen, by increasing the tilt angle for a fixed value of wavelength, $\text{Re}(n_{\text{eff}})$ would decrease. By decreasing the effective refractive index, the Fabry-Perot (F-P) resonances of propagating plasmon modes occur in shorter slits. In Figure 3(a), only the centric slit achieves the F-P resonance when $\phi = 0°$ which makes the focus closer to the exit surface. When the tilt angle increases to $\phi = 45°$, the decrease of $\text{Re}(n_{\text{eff}})$ causes the two slits on the both sides of the centric slit to achieve F-P resonance. Thus, the focal length increases as shown in Figure 3(b). If the tilt angle continues to increase to $\phi = 90°$, the two outermost slits achieve F-P resonance instead of the other slits; therefore, it is expected that the focal length would increase. However, because of the convex profile, the depth of these two outermost slits is much smaller than the the depth of other slits and, consequently, the focus moves closer to the exit surface in compare with

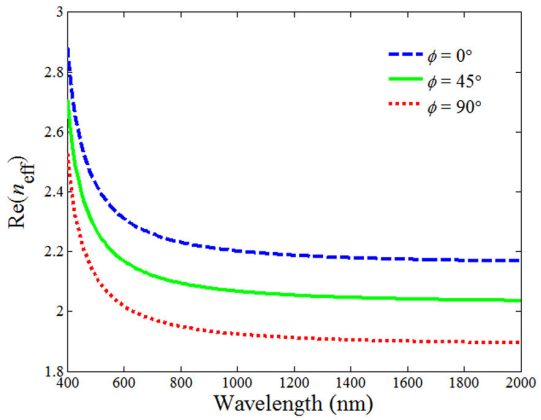

FIG. 4 Real Part of effective refractive index versus wavelength for $\phi = 0°$ (blue dashed curve), $\phi = 45°$ (green solid curve) and $\phi = 90°$ (red dotted curve).

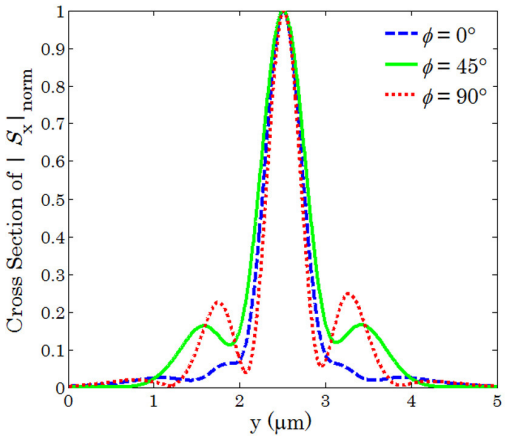

FIG. 5 Comparison between calculated cross sections of the normalized amplitude of the x-component of the time averaged Poynting Vector, $|S_x|$, at the focal point for $\phi = 0°$ (blue dashed curve), $\phi = 45°$ (green solid curve) and $\phi = 90°$ (red dotted curve).

$\phi = 45°$, but the focal length is still larger than the one at $\phi = 0°$.

A monitor line has been used to record the intensity level of the beam. The calculated cross sections of amplitude of the x-component of the time averaged Poynting Vector, $|S_x|$, are illustrated in Figure 5 for $\phi = 0°$, $\phi = 45°$ and $\phi = 90°$. The focused spot size at $\phi = 0°$, $\phi = 45°$ and $\phi = 90°$ are about 495 nm, 600 nm and 425 nm, respectively.

The focal length and also the transmittance through the lens versus tilt angle diagrams are also illustrated in Figure 6. The maximum tuning range of the focal length by the applied electric field occurs for a change in tilt angle from $\phi = 0°$ to $\phi = 45°$ and its value is about 725 nm.

Our simulations demonstrate the feasibility of beam focusing with the use of nano-slit array whose geometry is properly shaped to induce a phase correction at the exit surface. Optimization of the structure geometry should lead to improved performance.

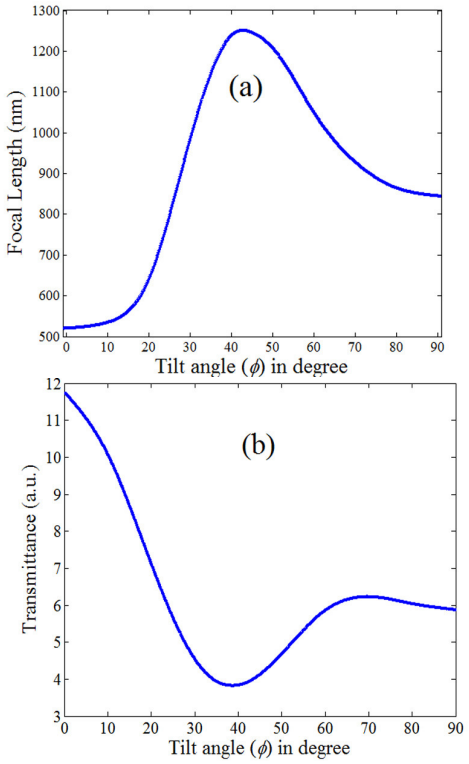

FIG. 6 (a) The focal length versus tilt angle (b) The transmittance versus tilt angle

5 CONCLUSION

Summarizing, we have numerically proposed a tunable plasmonic lens based on Metal-Anisotropic-Metal (MAM) structure. By application of an external electric field, the orientation of the LC molecules can be controlled, thus, inducing a variation of the refractive index which, in turn, leads to a change in SP modes. The simulated results clearly show that the focal point can be controlled easily. Moreover, large tuning range of the focal length up to 725 nm can be achieved. In fact, the active control of beam in plasmonic lens has great applications in near-field scanning, SPs antenna, etc.

6 ACKNOWLEDGMENTS

The authors would like to thank Dr. Sogand Noroozizadeh for many stimulating discussions.

References

[1] W. L. Barnes, A. Dereux, and T. W. Ebbesen, "Surface plasmon subwavelength optics," Nature **424**, 824-830 (2003).

[2] T. W. Ebbesen, H. J. Lezec, H. F. Ghaemi, T. Thio, and P. A. Wolff, "Extraordinary optical transmission through sub-wavelength hole arrays," Nature **391**, 667-669 (1998).

[3] S. I. Bozhevolnyi, V. S. Volkov, E. Devaux, J. Y. Laluet, and T. W. Ebbesen, "Channel plasmon subwavelength waveguide components including interferometers and ring resonators," Nature **440**, 508–511 (2006).

[4] L. Verslegers, P. B. Catrysse, Z. Yu, J. S. White, E. S. Barnard, M. L. Brongersma, and S. Fan, "Planar Lenses Based on Nanoscale Slit Arrays in a Metallic Film", Nano Lett. **9 (1)**, 235 (2009).

[5] Z. Sun, and H. K. Kim, "Refractive transmission of light and beam shaping with metallic nano-optic lenses," Appl. Phys. Lett. **85**, 642–644 (2004).

[6] H. Shi, C. Wang, C. Du, X. Luo, X. Dong, and H. Gao, "Beam manipulating by metallic nano-slits with variant widths," Opt. Express **13**, 6815–6820 (2005).

[7] L. Lin, X. M. Goh, L. P. McGuinness, and A. Roberts, "Plasmonic lenses formed by two-dimensional nanometric cross-shaped aperture arrays for Fresnel-region focusing," Nano Lett. **10 (5)**, 1936–1940 (2010).

[8] G. G. Zheng, and X. Y. Li, "Optical beam manipulation through two metal subwavelength slits surrounded by dielectric surface gratings," J. Opt. A - Pure Appl. Opt. **11 (7)**, 075002 (2009).

[9] E. Ozbay, "Plasmonics: Merging Photonics and Electronics at Nanoscale Dimensions," Science **311**, 189–193 (2006).

[10] D. D. Ceglia, M. A. Vincenti, and M. Scalora, "Wideband plasmonic beam steering in metal gratings," Opt. Lett. **37**, 271–273 (2012).

[11] C. Min, P. Wang, X. Jiao, Y. Deng, and H. Ming, "Beam manipulating by metallic nano-optic lens containing nonlinear media," Opt. Express **15**, 9541–9546 (2007).

[12] M. A. Vincenti, A. D'Orazio, M. Buncick, N. Akozbek, M. J. Bloemer, and M. Scalora, "Beam steering from resonant subwavelength slits filled with a nonlinear material," JOSA B **26**, 301–307 (2009).

[13] C. C. Lee, C. Mohr, J. Bethge, S. Suzuki, M. E. Fermann, I. Hartl, and T. R. Schibli, "Frequency comb stabilization with bandwidth beyond the limit of gain lifetime by an intracavity graphene electro-optic modulator," Opt. Lett. **37**, 3084–3086 (2012).

[14] Y. Shao, W. Qin, H. Liu, J. Qu, X. Peng, H. Niu, and B. Z. Gao, "Ultrafast, large-field multiphoton microscopy based on an acousto-optic deflector and a spatial light modulator," Opt. Lett. **37**, 2532–2534 (2012).

[15] P. Li, T. Sasaki, L.F. Pan, and K. Hane, "Comb-drive tracking and focusing lens actuators integrated on a silicon-on-insulator wafer," Opt. Express **20**, 627–634 (2012).

[16] X. Wang, B. Wang, P. J. Bos, P. F. McManamon, J. J. Pouch, F. A. Miranda, and J. E. Anderson, "Modeling and design of an optimized liquid-crystal optical phased array," J. Appl. Phys. **98**, 073101–073101-8 (2005).

[17] W. Dickson, G. A. Wurtz, P. R. Evans, R. J. Pollard, and A. V. Zayats, "Electronically controlled surface plasmon dispersion and optical transmission through metallic hole arrays using liquid crystal," Nano Lett. **8 (1)**, 281 (2008).

[18] V. K. S. Hsiao, Y. B. Zheng, B. K. Juluri, and T. J. Huang, "Light-Driven Plasmonic Switches Based on Au Nanodisk Arrays and Photoresponsive Liquid Crystals," Adv. Mater. **20**, 3528–3532 (2008).

[19] P. R. Evans, G. A. Wurtz, W. R. Hendren, R. Atkinson, W. Dickson, A. V. Zayats, and R. J. Pollard, "Electrically switchable nonreciprocal transmission of plasmonic nanorods with liquid crystal," Appl. Phys. Lett. **91**, 043101 (2007).

[20] A. C. Tasolamprou, D. C. Zografopoulos, and E. E. Kriezis, "Liquid crystal-based dielectric loaded surface plasmon polariton optical switches," J. Appl. Phys. **110**, 093102-1–9 (2011).

[21] M. Bahramipanah, M. S. Abrishamian, and S. A. Mirtaheri, "Tunable anisotropic photonic crystal channel-drop filter," J. Opt. **13**, 015103-1–8 (2011).

[22] M. Dridi, and A. Vial, "FDTD Modeling of Gold Nanoparticles in a Nematic Liquid Crystal: Quantitative and Qualitative Analysis of the Spectral Tunability," J. Phys. Chem. C **114**, 9541–9545 (2010).

[23] M. Bahramipanah, S. A. Mirtaheri, and M. S. Abrishamian, "Electrical beam steering with metal-anisotropic-metal structure," Opt. Lett. **37 (4)**, 1–3 (2012).

[24] P. A. Kossyrev, A. Yin, S. G. Cloutier, D. A. Cardimona, D. Huang, P. M. Alsing, and J. M. Xu, "Electric field tuning of plasmonic response of nanodot array in liquid crystal matrix," Nano Lett. **5**, 1978–1981 (2005).

[25] L. Dou, and A. R. Sebak, "3D FDTD method for arbitrary anisotropic materials", Microw. Opt. Techn. Let. **48**, 2083–2090 (2006).

[26] W. H. P. Pernice, F. P. Payne, and D. F. G. Gallagher, "An FDTD method for the simulation of dispersive metallic structures," Opt. Quant. Electron. **38**, 843–856 (2006).

[27] A. Taflove, and S. C. Hagness, *Computational Electrodynamics: The Finite-Difference Time-Domain Method,* (Artech House, Norwood (MA), 2005).

[28] J. Tao, X. G. Huang, X. Lin, Q. Zhang, and X. Jin, "A narrow-band subwavelength plasmonic waveguide filter with asymmetrical multiple-teeth-shaped structure," Opt. Express **17**, 13989–13994 (2009).